Influence of the chemical structure of polyester polyols on the properties and fire resistance of polyisocyanurate foams

Antoine Duval, Johan Sarazin, Cecile de Haas, Alexandru Sarbu, Serge Bourbigot, Luc Avérous

European Polymer Journal 210 (2024) 112938

Contents lists available at ScienceDirect

European Polymer Journal

journal homepage: www.elsevier.com/locate/europolj

Influence of the chemical structure of polyester polyols on the properties and fire resistance of polyisocyanurate foams

Antoine Duval [a,b,*], Johan Sarazin [c], Cecile de Haas [a], Alexandru Sarbu [a,b], Serge Bourbigot [c,d], Luc Avérous [a]

[a] BioTeam/ICPEES-ECPM, UMR CNRS 7515, Université de Strasbourg, 25 rue Becquerel, 67087, Strasbourg Cedex 2, France
[b] Soprema, 15 rue de Saint Nazaire, 67100 Strasbourg, France
[c] Univ. Lille, CNRS, INRAE, Centrale Lille Institut, UMR 8207, UMET, Unité Matériaux et Transformations, F-59000 Lille, France
[d] Institut Universitaire de France, Paris, France

ARTICLE INFO

Keywords:
Polyisocyanurate
Foam
Thermal insulation
Polyester polyols
Aromaticity

ABSTRACT

Polyisocyanurate foams are high-performance thermal insulation materials widely used in the building industry. They combine low thermal conductivity with good fire resistance, thanks to the presence of isocyanurate structures. The impact of the chemical structure of their main building block, polyester polyols, has however rarely been the topic of a systematic investigation. In this work, a series of polyester polyols was synthesized from phthalic anhydride and various diols, resulting in polyols having a constant hydroxyl index but varying levels of aromaticity. Their viscosity and glass transition temperature were found to increase with the aromaticity. The polyols were then used to synthesize rigid polyisocyanurate foams for thermal insulation, to evidence the impact of aromaticity on the properties and fire resistance of the foams. Increasing the polyol aromaticity limits the molecular mobility, which results in slower foaming reaction times. The differences in reactivity between the polyols also lead to foams with slightly different isocyanurate contents, although they were all synthesized with a constant NCO/OH ratio. The main foam properties (morphology, mechanical properties or thermal conductivity) were mostly unaffected by the polyol aromaticity. The aromaticity was not found to improve the fire behavior of the foams, as evidenced by mass loss cone experiments. However, other factors, such as the isocyanurate content of the foams and the oxygen content of the polyols were found to positively influence the fire resistance. It should be related to a higher propensity to form a dense char layer on top of the material, limiting its degradation during the combustion.

1. Introduction

With the growing concern to reduce energy consumption and greenhouse gas emissions, thermal insulation has become a key focus of attention in the construction field for a more sustainable future. Indeed, one third of the worldwide energy is consumed for heating or cooling buildings [1]. With a thermal conductivity below 25 mW m^{-1} K^{-1}, rigid polyurethane foams are among the most efficient thermal insulating materials, and are widely used by the building industry [2,3]. Two types of rigid polyurethane foams can be distinguished, depending on the chemical architecture of the polymer network. Polyurethane (PUR) foams are based on urethane linkages, formed by the reaction between polyisocyanates and polyols, whereas polyisocyanurate (PIR) foams are mostly based on isocyanurate linkages formed by the trimerization of isocyanates (Scheme 1) [4].

The tragic fire of the Grenfell Tower in London in 2017 shed lights on the importance of the fire behavior of façade materials [5], including PIR insulation foams [6]. PIR foams have a much better fire resistance than PUR foams and have therefore progressively supplanted the latter because of the stringent requirements of the building industry. The reaction to fire of PIR depends on the presence of isocyanurate rings, which are more thermally stable than urethane linkages [7]. The higher thermal stability of the isocyanurate linkage limits the release of polyol during combustion, which further degrades into small volatile flammable fragments [8]. In addition, the rigid crosslinked structure provided by the isocyanurate linkages favors the formation of a dense and continuous char layer, which restricts the diffusion of volatile species and protects the polymer from further degradation [8,9].

* Corresponding author at: BioTeam/ICPEES-ECPM, UMR CNRS 7515, Université de Strasbourg, 25 rue Becquerel, 67087, Strasbourg Cedex 2, France.
E-mail address: antoine.duval@unistra.fr (A. Duval).

https://doi.org/10.1016/j.eurpolymj.2024.112938
Received 10 January 2024; Received in revised form 13 March 2024; Accepted 14 March 2024
Available online 15 March 2024

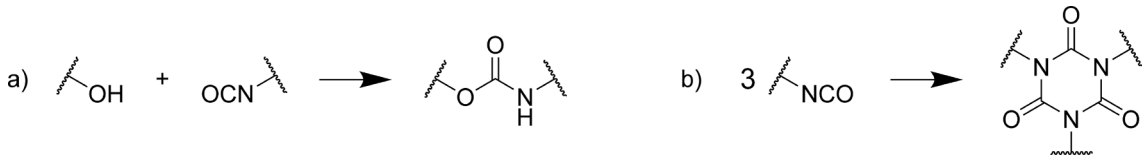

Scheme 1. Synthesis of (a) urethanes by reaction between isocyanate and alcohols and (b) isocyanurates by trimerization of isocyanates.

Flammability of PIR foams is directly correlated to the content in isocyanurate rings, which depends on the content and nature of the trimerization catalyst, the index of the formulation (*i.e.*, the NCO/OH molar ratio) and the polyol equivalent weight [10–12]. Foams prepared with a high index present the best fire resistance, but to the cost of poor mechanical properties, such as a high brittleness. The need for compromises between fire resistance and other properties has thus led to a reduction of the index of PIR foams, which are sometimes referred to as urethane-modified PIR. To compensate for the resulting loss in fire behavior, flame retardants (FRs) can be incorporated. In addition, the ban of chlorofluorocarbon (CFC) blowing agents in the 1990's and their replacement by highly flammable pentanes has caused an important increase in PIR foams flammability, which had to be counterbalanced by the incorporation of more FRs [13]. Many different FRs have been tested in PIR foams, including halogenated FRs (chlorinated, brominated) [14,15], halogen-free phosphorous-based FRs [16–20], intumescent expandable graphite [20–23], aluminum hydroxide [24,25], nanoclays [26,27] and synergistic combinations of various types of FRs [24–29].

For PIR formulations, changing the catalyst or adjusting its concentration can favor the trimerization of isocyanates into isocyanurates, thus leading to improved fire behavior [30,31]. However, PIR foams are heterogeneous materials. Reignier et al. elegantly evidenced the existence of a chemical gradient within PIR foams using FTIR spectroscopy [32]. They found that within a foam panel, the fire resistance is correlated to the proportion of isocyanurate rings, which increases from surface to core. The chemical gradient is a consequence of the thermal gradient occurring during foam formation: the temperature is highest in the core because heat loss is minimized thanks to the intrinsic thermal insulation properties of the foam [32].

The aromaticity of the polyol is usually thought to positively influence the reaction to fire. Substitution of aliphatic polyether polyols by aromatic polyester polyols resulted in an improvement of the flame performance in PUR foams [33]. However, there was almost no difference in limiting oxygen index (LOI) for PIR foams prepared from aliphatic or aromatic polyester polyols [34]. In addition, polyols based on secondary OH groups result in foams with higher flammability, which can be related to a higher hydrogen content of the polyol caused by the extra methyl group, leading to the release of more flammable gases during the combustion [10].

However, there has not been any systematic evaluation of the influence of polyol aromaticity on the fire performance of PIR foams. The aim of this study is thus to understand the impact of the aromaticity of one of the main building block, the polyester polyols, on the properties and reaction to fire of PIR foams. A series of polyester polyols was synthesized from phthalic anhydride and diols of various lengths, yielding polyols of similar OH-value (I_{OH} = 240–250 mg KOH g^{-1}) but with different degrees of aromaticity. The polyols were characterized by chemical titration, FTIR, NMR, DSC, and rheology. They were then used to prepared PIR foams with a constant index of 320, in the presence or absence of a halogenated FR, tris(1-chloro-2-propyl) phosphate (TCPP). The main properties of the foams were studied, such as morphology, closed cells content, dimensional stability, mechanical properties, and thermal conductivity. The fire behavior was finally evaluated by mass loss cone experiments.

Table 1
The different short diols used in polyester polyols synthesis.

Diol	Abbreviation	M (g/mol)	bp (°C)	I_{OH} (mg KOH g^{-1})
Ethylene glycol	MEG	62.1	197	1808
Diethylene glycol	DEG	106.1	245	1057
Triethylene glycol	TEG	150.2	285	747
1,3-propanediol	PDO	76.1	213	1475
Dimer of 1,3-propanediol	DPDO	134	> 300	837
1,6-hexanediol	HDO	118.2	250	949

2. Materials and methods

2.1. Materials

Ethylene glycol (MEG, 99 %), diethylene glycol (DEG, 99 %) triethylene glycol (TEG, 99 %), 1,3-propanediol (PDO, 99 %) hexanediol (HDO, 97 %) and phthalic anhydride (PA, 99 %) were purchased from Alfa Aesar. Dimer of 1,3-propanediol (DPDO, 3-(3-hydroxypropoxy) propan-1-ol) was obtained from Weylchem under the brand name Velvetol® H134. Titanium isopropoxide (TTIP) was purchased from Sigma-Aldrich.

For the foam formulations, polymeric 4,4′-methylene bis-(phenyl isocyanate) (pMDI, Lupranat M 70 R, BASF), was used as aromatic polyisocyanate. It has an NCO content of 31 % and an average functionality of 2.9. Polyether – polydimethylsiloxane copolymer (Tegostab B1048, Evonik) was used as surfactant. N,N'-dimethylcyclohexylamine (DMCHA, Sigma-Aldrich) and potassium *iso*-octanoate (K-Zero 3000, Momentive) were used as catalysts. Tris(1-chloro-2-propyl) phosphate (TCPP, Shekoy Chemicals) was used as FR, and isopentane (Inventec-Dehon) was used as physical blowing agent.

2.2. Polyester polyols synthesis

Polyester polyols were synthesized with a target I_{OH} of 250 mg KOH g^{-1}. Different short diols were reacted with PA, with a controlled molar ratio of diol to PA to theoretically obtain the target I_{OH}. The diols used and their properties are listed in Table 1.

The total initial mass was set to 1800 g. Diol, PA and TTIP (0.18 g, 100 ppm) were introduced in a 3 L glass reactor equipped with a mechanical stirrer, a thermocouple, a nitrogen inlet and a Dean-Stark trap topped with a condenser to recover the water produced during the reaction. The temperature was initially set to 175 °C and then gradually raised to 220 °C under constant stirring. Aliquots were withdrawn at regular intervals to measure the acid value (I_A). When the measured I_A was below 10 mg KOH g^{-1}, the Dean-Stark trap was replaced by a short path distillation column connected to a vacuum pump. The pressure was progressively lowered to about 700–800 mbar to allow the esterification to proceed further. Aliquots were withdrawn to measure the I_A, and the reaction was stopped when I_A < 1.5 mg KOH g^{-1}. The I_{OH} of the polyol was measured, and diol was added to compensate for evaporation losses and achieve the target I_{OH}. The polyester polyols are labelled as PA-XXX, where XXX stands for the abbreviation of the corresponding diol (Table 1).

Table 2
Formulations of the PIR foams.

Component	Name	Quantity
Polyester polyol	PA-XXX	
Polyisocyanate	pMDI	adjusted to index 320
Surfactant	Tegostab B81048	0.67 %wt
Catalyst	DMCHA	0.24 %wt
Catalyst	Potassium octanoate	0.81 %wt
Blowing agent	isopentane	12.6 %wt
Blowing agent	water	0.24 %wt
Flame retardant	TCPP	0 or 5.8 %wt

2.3. Preparation of PIR foams

PIR foams were prepared with the synthesized polyester polyols and pMDI, with a constant index of 320. The formulations are given in Table 2. A blend containing polyol, catalysts, surfactant, FR and water was first prepared. The mixture was mechanically stirred at 9000 rpm for 1–2 min before incorporating the blowing agent. As discussed in the Results section, some of the prepared polyester polyols had a high viscosity and required heating up to 40 °C to ensure proper mixing. Isopentane was then added, and the mixture was stirred with a progressive increase in speed up to 5000 rpm, until obtaining a fine white emulsion with the incorporation of the correct amount of blowing agent. The temperature of the premix was adjusted to 20 °C. Then, the right amount of polyisocyanate was quickly added with a syringe, and the mixture was vigorously stirred for 5 s at 7500 rpm. The mixture was then poured into the container of the Foamat device (cylinder of 15 cm diameter and 18 cm height) or into a square mold (30 × 30 × 60 cm^3) for the preparation of bigger samples. Foams were conditioned 7 days prior to cutting samples for the different analyses.

2.4. Polyester polyols characterizations

I_{OH} and I_A were measured by titration with an automatic titrator, following standard procedures.

NMR was performed on a Bruker 400 MHz spectrometer. For ^1H NMR, approximately 20 mg of sample were dissolved in 600 µL of $CDCl_3$. 16 scans were recorded at 25 °C. ^{31}P NMR was used to measure the I_{OH} of the polyols and compare with the data obtained by titration. About 30 mg of polyester polyols was derivatized with 2-chloro-4,4,5,5-tetramethyl-1,3,2-dioxaphospholane in pyridine/$CDCl_3$ (1.6:1 v/v) in the presence of cholesterol as internal standard, according to standard protocol [35,36]. 128 scans were recorded with 15 s relaxation delay. The hydroxyl index I_{OH} was calculated according to Eq. (1):

$$I_{OH}\left(mg\ KOH\ g^{-1}\right) = [OH] \times 56.1 \quad (1)$$

where *[OH]* is the polyol content in OH groups measured by ^{31}P NMR (in mmol/g) and 56.1 is the molar mass of KOH (in g/mol)

Fourier Transformed Infrared (FTIR) spectroscopy was performed on a ThermoScientific Nicolet iS10 spectrometer equipped with a diamond ATR probe. 32 scans were collected at room temperature at a resolution of 4 cm^{-1}.

Viscosity measurements were performed on a TA Discovery HR-3 rheometer equipped with Peltier plates at 25 °C, using 25 mm parallel plate geometry, for shear rates ranging from 0.1 to 100 s^{-1}, where a Newtonian behavior was observed.

Differential Scanning Calorimetry (DSC) was performed on a Discovery DSC-25 apparatus from TA instruments. The samples were first equilibrated at 120 °C for 3 min, then cooled down to –80 °C at a cooling rate of 10 °C min^{-1} and kept 1 min at this temperature. Finally, they were heated up to 100 °C at 10 °C min^{-1}. Glass transition temperature (T_g) was measured as the slope change during the heating run.

Size-exclusion chromatography (SEC) was performed on a Waters Acquity Advanced Polymer Chromatography (APC) system, equipped with three 150-mm APC XT columns (a 45 Å, 1.7 µm column; a 200 Å, 2.5 µm column; and a 450 Å, 2.5 µm column) regulated at 40 °C. Tetrahydrofuran (THF, HPLC grade, Fisher Scientific) was used as the eluent at a flow rate of 0.6 mL min^{-1}. Detection was performed with a refractive index (RI) detector and a tunable UV detector operating at 280 nm. The samples were dissolved in THF at 5 mg mL^{-1} and filtered through 0.2 µm PTFE syringe filters prior to the injection. The average molar masses and dispersities were calculated from a calibration with polystyrene standards.

2.5. Characterization of PIR foams

To follow the foaming process, the core temperature, foam height and expansion rate were continuously recorded using a Foamat® FPM 150 device (Messtechnik GmbH, Germany). The apparatus was equipped with a cylindrical container (15 cm diameter and 18 cm height), an ultrasonic probe to record the foam height, a platinum sensor to follow the temperature evolution inside the foam, and a pressure sensor located at the bottom of the cylindrical container.

Apparent foam density was measured by weighing parallelepipedal foam samples whose dimensions were measured with a caliper, according to EN 1602 standard. Dimensional stability was measured after 48 h at 70 °C and 90 % humidity rate, and after 48 h at −20 °C, according to EN 1604 standard. Compression strength at 10 % deformation was measured on 100 × 100 × 60 mm^3 foam samples with an Instron 3367 dynamometer equipped with a 30 kN load sensor at room temperature, according to EN 826 standard. Closed cells content was determined using a gas pycnometer (Ultrapyc 1200e, Quantachrome Instruments), according to EN ISO 4590 standard. Cubic foam samples (approximately 25 × 25 × 25 mm^3) were used for the first measurement. They were then cut into eight smaller and equivalent pieces and a second measurement was performed to correct the closed cells content from the closed cells that were opened during the cutting step. Scanning electron microscopy (SEM) was carried out to determine the cells size distribution using a Jeol IT-100 equipment and an in-house statistical imaging analysis software based on Image J. Cubic foam samples were cut with a microtome blade and analyzed in longitudinal (*i.e.*, parallel to foam rise) and transverse (*i.e.*, perpendicular to foam rise) directions. Thermal conductivity was measured 7 days after foaming with a heat flowmeter (HFM 446, Netzsch), according to EN 12939 standard. Foam samples of 175 × 175 × 60 mm^3 were analyzed at 20 °C to determine the thermal conductivity coefficient λ.

2.6. Thermal and flammability analyses of PIR foams

Thermogravimetric analyses (TGA) were performed on a TA Instrument Hi-Res TGA Q5000. Foam samples were heated from room temperature to 700 °C at a heating rate of 20 °C min^{-1} under helium. To evaluate the influence of the polyol structure, the residual mass at 700 °C (m_{res}) and the temperature at which 95 % of the initial remains ($T_{95\%}$) were determined.

Flammability tests were performed according to EN ISO 11925–2 standard, measuring the maximum flame height on the sample after exposition for 15 s to a direct flame.

Mass Loss Cone (MLC) was performed on an equipment from Fire Testing Technology (FTT), following the procedure defined in the ASTM E 906 standard. The equipment is identical to that used in oxygen consumption cone calorimetry (ASTM E-1354–90), with the difference that a thermopile in the chimney is used to obtain the Heat Release Rate (HRR) instead of the oxygen consumption principle. The foam samples (100 × 100 × 20 mm^3) were exposed to a horizontal heat flux. The external heat flux was set at 35 kW m^{-2}, corresponding to a common heat flux in a moderate fire scenario [37,38]. The HRR, peak HRR (pHRR), and Total Heat Released (THR) were measured with a reproducibility of ± 10 %, the ignition with a reproducibility of ± 15 %.

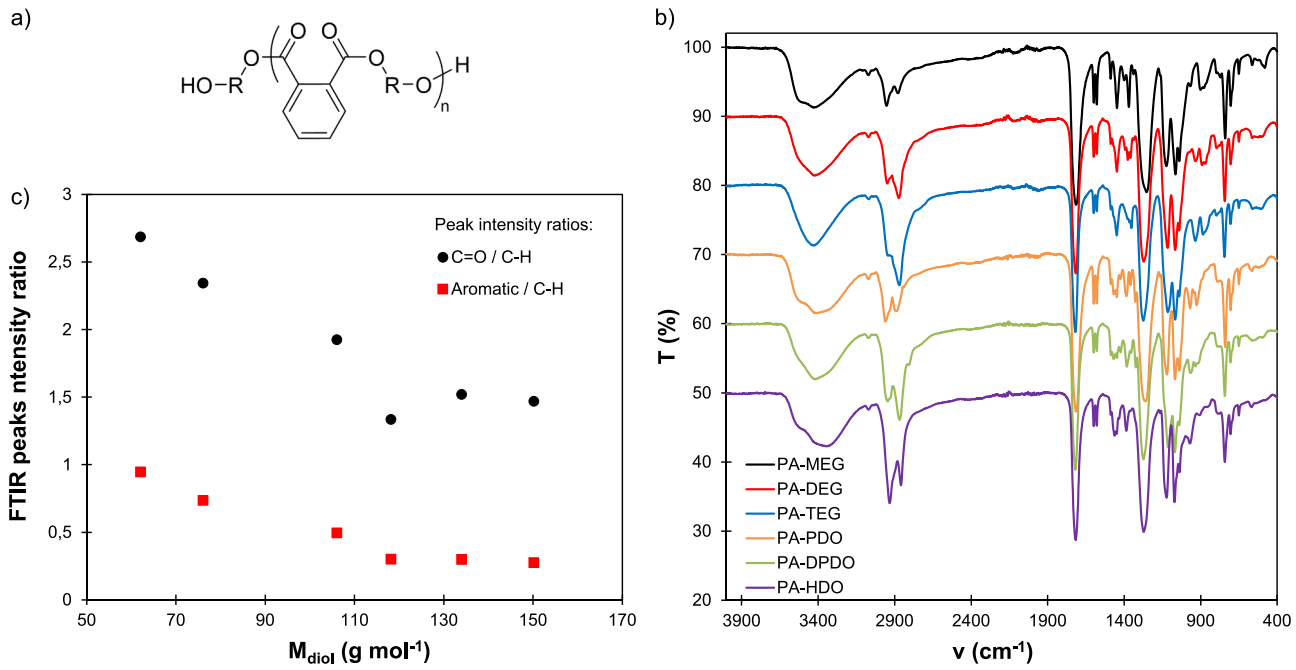

Fig. 1. (a) Structure of the synthesized polyester polyols, (b) ATR-FTIR spectra and (c) ratio of the intensity of FTIR bands of the polyols.

Table 3
I_{OH} and I_A values of the synthesized polyester polyols.

Polyester polyol	I_{OH} (mg KOH g^{-1})		I_A (mg KOH g^{-1})	
	by titration	by ^{31}P NMR	by titration	by ^{31}P NMR
PA-MEG	257	252	0.9	nd
PA-DEG	248	262	0.7	0.5
PA-TEG	247	258	1.3	0.6
PA-PDO	249	246	0.5	nd
PA-DPDO	239	252	0.5	nd
PA-HDO	249	256	0.9	1.3

nd = not detected.

3. Results and discussion

3.1. Synthesis and characterization of polyester polyols with varying aromaticity

A series of 6 polyester polyols was synthesized from the reaction between PA and various diols, listed in Table 1. Their theoretical structure is given in Fig. 1a. The proportion between PA and diols was adjusted to obtain polyester polyols with similar I_{OH}, meaning that they also present similar average molar masses. The I_{OH} and I_A of the polyols are summarized in Table 3. They have been measured by titration and ^{31}P NMR, which gave comparable results. ^{31}P NMR spectra are available as supporting information (Figs. S1 and S2). All the polyester polyols have similar I_{OH}, ranging from 239 to 257 mg KOH g^{-1}. The I_A are below 1.5 mg KOH g^{-1}. In most cases, carboxylic acid groups could not be detected by ^{31}P NMR because of their low abundance. SEC confirmed that all polyols present similar molar mass distributions (Fig. S3).

^{1}H NMR confirmed the expected structures of the polyester polyols (Figs. S4 to S9). FTIR spectra of the polyols show the characteristic absorption bands of polyester polyols: large O-H stretch centered around 3400 cm^{-1}, C-H bands at 2860 and 2930 cm^{-1}, an intense C=O stretch band relative to ester bonds at 1715 cm^{-1} and two sharp peaks at 1580 and 1600 cm^{-1} corresponding to the aromatic C-H (Fig. 1b).

The ratios between the intensity of selected peaks have been plotted against the diol molar mass on Fig. 1c. The C=O/C-H ratio, which is proportional to the quantity of ester bonds in the polyol, decreases when the diol length increases, as expected. The aromatic/C-H ratio follows the same trend, showing that the aromaticity of the polyols decreases when increasing the diol molar mass.

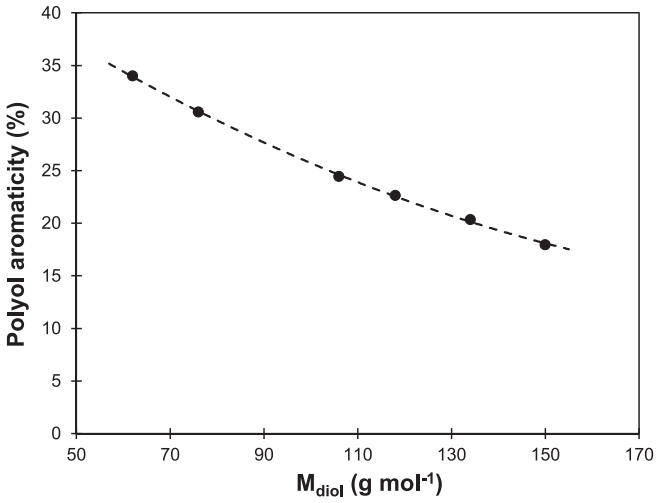

Fig. 2. Aromaticity of polyester polyols, calculated from Equation (2), depending on the molar mass of the diols used in the synthesis.

Polyol aromaticity was then calculated from Eq. (2), based on their chemical structures. Details of the calculation are available in SI. The aromaticity is directly correlated to the diol molar mass (Fig. 2).

$$Aromaticity(mol\%) = 100 \times \frac{M_{aromatic}}{M_{total}} \quad (2)$$

with $M_{aromatic}$ the molar mass of the aromatic ring of the repeating unit (76 g mol^{-1}) and M_{total} the molar mass of the repeating unit.

The calculated aromaticity has also been compared to an aromaticity ratio measured by ^{1}H NMR. The details of its calculation are available in SI. Both data are correlated but do not perfectly match (Fig. S10), because the aromaticity ratio measured by ^{1}H NMR only considers –CH- and –CH_2- groups, whereas the aromaticity calculated from Eq. (1) also

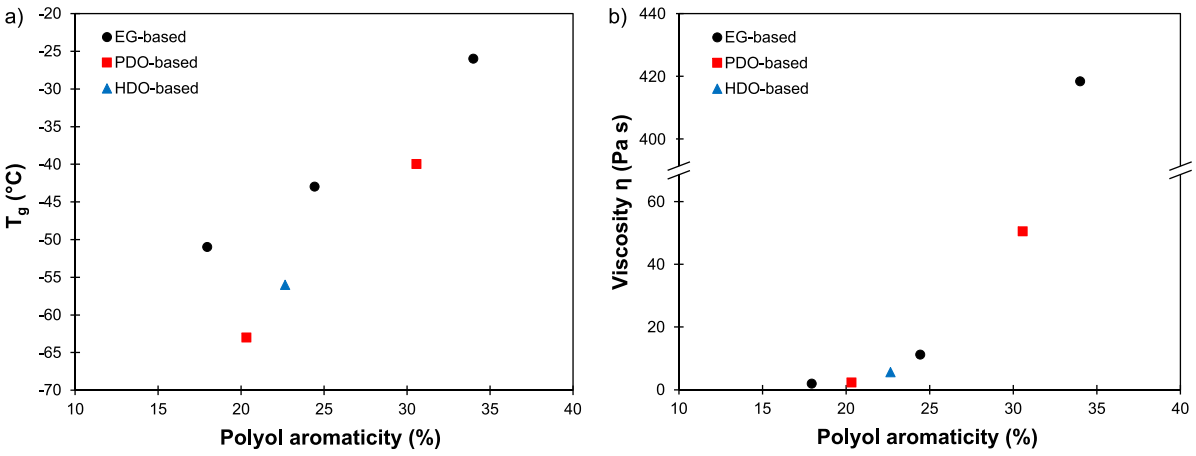

Fig. 3. Evolutions of (a) T_g and (b) viscosity at 25 °C of polyester polyols depending on their aromaticity.

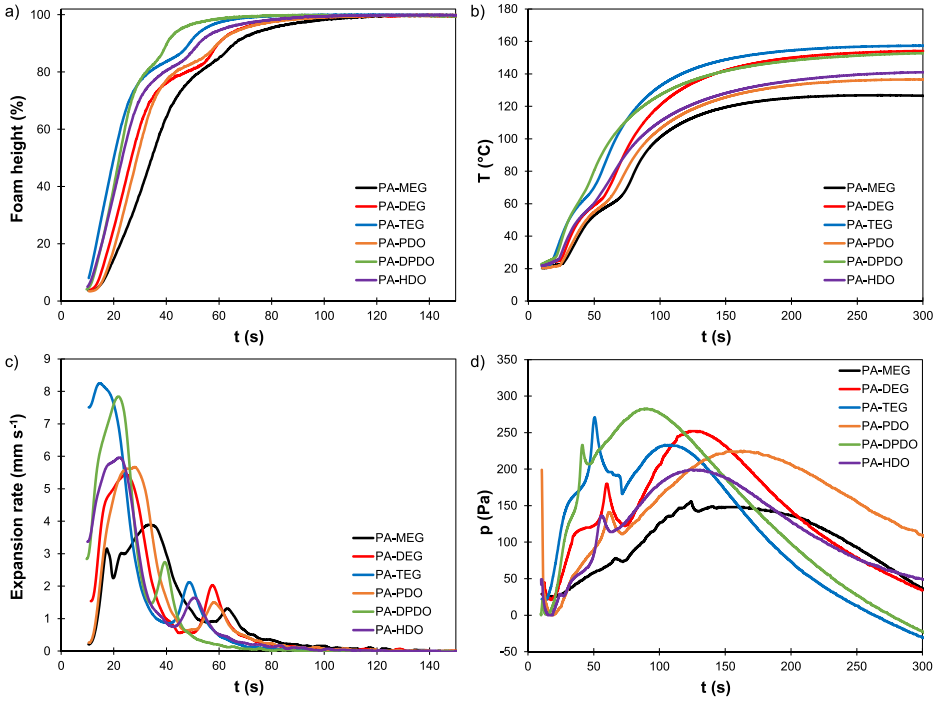

Fig. 4. (a) Foam height, (b) temperature inside the foam, (c) expansion rate and (d) pressure measured during foam formation, depending on the nature of the polyester polyol, for foam series prepared with FR.

takes into account the presence of –COO- ester groups and quaternary carbons in the polyols.

The properties of the polyols were then examined with respect to their aromaticity. T_g was determined by DSC. Thermograms are available in SI (Figs. S11 and S12). T_g was logically found to increase with the polyol aromaticity, because aromatic groups bring rigidity to the polymer chains (Fig. 3a). Increasing aromaticity also results in a notable increase of the polyols viscosity (Fig. 3b). For PA-MEG, an elevated viscosity is obtained (>400 Pa s), which compromises its use for foam applications. PA-PDO also presents a high viscosity (about 50 Pa s) and may be difficult to use in foams, whereas the other polyols present lower viscosities (between 2 and 11 Pa s) and are thus compliant to the requirements.

3.2. *Influence of polyester polyols structure on the foaming kinetics*

Two series of PIR foams were prepared with the different polyols. Their formulations are given in Table 2. The amounts of catalysts and blowing agent were maintained constant based on the total formulation weight. One series was prepared with FR and another one without, to later evaluate its influence on the fire resistance. The used FR is a low viscosity liquid, which therefore also acts as viscosity reducer of the mixture, facilitating the processing. In the absence of FR, it was not possible to obtain foams with PA-MEG as polyol, because of its excessive viscosity.

The foaming kinetics was followed by recording the foam height, expansion rate, temperature, and bottom pressure throughout the foaming process. Data are presented in Fig. 4 for the foam series containing FR. Foam height and expansion rate are only presented up to 150 s, because they don't evolve significantly afterwards, whereas temperature and bottom pressure are shown up to 300 s.

The foam height increases in two different phases, as commonly observed for PIR foams [39]. Consequently, the expansion rate, which is the derivative of the height over time, presents two distinct peaks. The

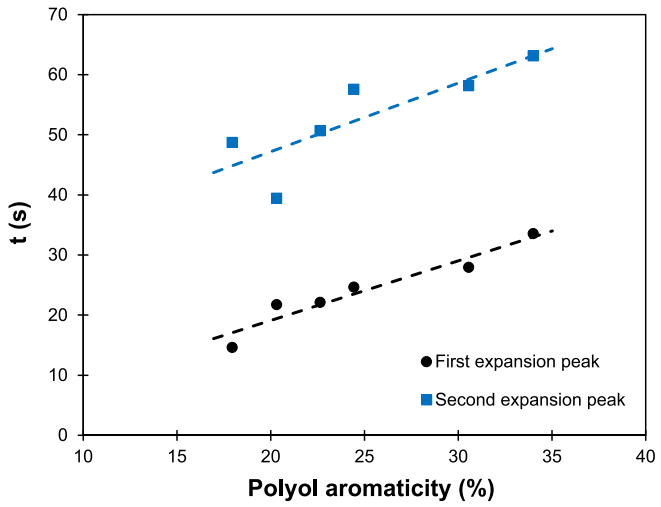

Fig. 5. Time to reach the expansion peaks during foam formation, depending on the polyester polyol aromaticity, for foam series prepared with FR.

first expansion corresponds to the formation of a polyurethane network, whereas the second expansion phase is related to the trimerization of isocyanates into isocyanurates. The evolution of the temperature inside the foams also reflects this 2-stage phenomenon.

The time to reach the two expansion peaks has been plotted against the polyol aromaticity in Fig. 5. It clearly shows that the foaming kinetics is dependent on the polyol aromaticity. Increasing polyol aromaticity reduces the molecular mobility, which causes a lower reactivity, and hence slower foaming kinetics. The slower foaming kinetics may also be related to the higher viscosity of the polyols with increasing aromaticity, as discussed earlier (Fig. 3b). The data recorded for the foam series prepared without FR are available in the SI (Figs. S14 and S15) and show similar trends.

3.3. *Influence of polyester polyols type on the foams chemical structure and properties*

FTIR spectroscopy was used to characterize the foam chemical structure. Spectra of the foam series prepared with FR are presented in Fig. 6, whereas those of the foams prepared without FR are available in the SI (Fig. S16). The spectra show the characteristic peaks associated with PIR networks: N-H stretching around 3360 cm^{-1}, C=O stretching at 1705 cm^{-1}, N-H bending at 1507 cm^{-1} and C-N stretching around 1410 cm^{-1} [32]. The N-H bands are relative to the urethane linkages, whereas the C=O band is more complex, as it contains contributions from the carbonyl groups of urethanes, isocyanurates, ureas, as well as from the esters of the polyols. The C-N stretching band at 1410 cm^{-1} is usually used to evidence the presence of isocyanurate rings, because it does not interfere with the C-N stretching in urethane linkages, which is rather found in the same region as the N-H bending band [32]. In addition, unreacted isocyanates are clearly visible at 2273 cm^{-1} (-N=C= O stretching).

The intensity of the -N=C=O stretching band, which is indicative of the amount of unreacted isocyanates groups, appears to be correlated to the polyol viscosity (Fig. 6b). Indeed, as the viscosity of the mixture increases, the mobility of the NCO groups is reduced, lowering their

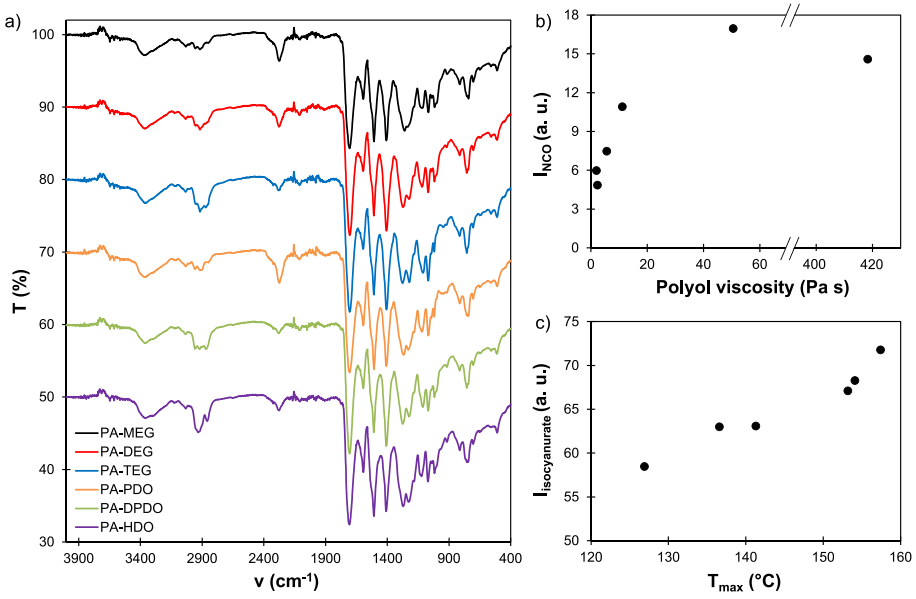

Fig. 6. A) ftir spectra of pir foams prepared with the different polyester polyols, b) evolution of the intensity of the nco band (2270 cm^{-1}) with the polyol viscosity, c) evolution of the isocyanurate band (1410 cm^{-1}) with the maximum temperature reached during foam formation, for foam series prepared with FR.

Table 4
Density, compression strength and dimensional stability of PIR foams prepared with the different polyester polyols.

Polyol	Density (kg m^{-3})	Compr. strength (kPa)	Dim. stab. at 70 °C, 90 %RH (%)			Dim. stab. at −20 °C (%)		
			length	width	thickness	length	width	thickness
PA-MEG	31.7	189	2.32	2.23	0.83	0.04	0.04	−0.04
PA-DEG	30.9	336	1.63	1.46	0.25	0.01	−0.07	−0.09
PA-TEG	31.1	343	1.24	1.27	0.17	0.07	0.04	0.11
PA-PDO	30.7	321	1.59	1.58	0.23	0.04	0.04	0.13
PA-DPDO	30.9	319	1.36	1.55	0.14	0.05	0.04	0.01
PA-HDO	31.3	330	1.54	1.69	0.18	−0.01	0.00	0.10

Table 5
Shore hardness, closed cells content, cells sizes and thermal conductivity of PIR foams prepared with the different polyester polyols.

Polyol	Shore 00	Closed cells (%)	Cells size (μm)		Therm. conductivity λ (mW m^{-1} K^{-1})
			diameter	height	
PA-MEG	62.4 ± 3.1	95	500 ± 130	700 ± 230	26.64
PA-DEG	74.0 ± 1.1	96	190 ± 50	360 ± 120	24.12
PA-TEG	72.5 ± 1.1	96	180 ± 50	320 ± 80	23.35
PA-PDO	71.7 ± 0.8	97	180 ± 50	340 ± 110	23.72
PA-DPDO	71.7 ± 0.9	97	170 ± 40	340 ± 90	23.35
PA-HDO	72.7 ± 1.9	96	180 ± 40	310 ± 90	23.63

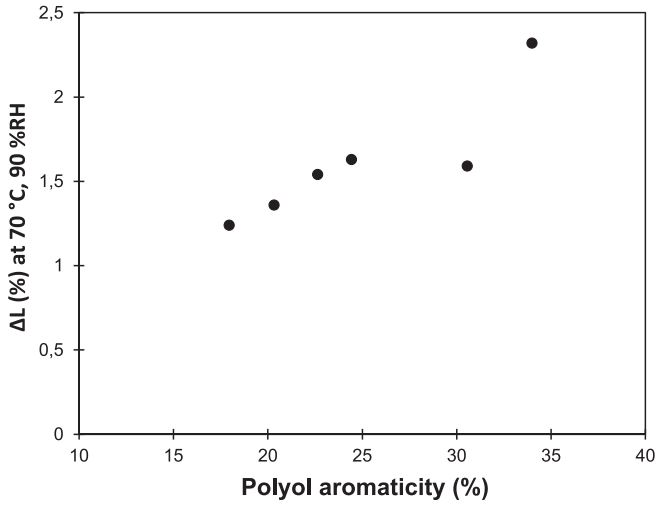

Fig. 7. Dimensional stability (evolution of sample length) at 70 °C, 90 %RH depending on the polyester polyol aromaticity.

reactivity.

The intensity of the isocyanurate band around 1410 cm^{-1} follows an opposite trend. To evaluate the content in isocyanurate in PIR panels, Reignier et al. divided the intensity of the isocyanurate peak by the intensity of the phenyl peak at 1595 cm^{-1} (aromatic C=C in-plane stretching vibration) [32]. In our case, the phenyl peak also contains the contribution of the aromatic groups of the polyols, which varies with its composition, as shown in Fig. 1. Such normalization was thus not possible, and only the intensity of the isocyanurate peak has been analyzed. As shown in Fig. 6c, it is well correlated with the maximum temperature reached during the foam expansion, obtained from the Foamat data (Fig. 4b). Indeed, high temperature is needed to achieve the trimerization of isocyanates into isocyanurates.

Only the foams containing FR were produced at larger scale and fully characterized. Their properties are listed in Table 4 and Table 5. Because of the excessive viscosity of the polyol, the foam prepared with PA-MEG presents poor structuration, and consequently poor properties. The sample has very large cells, leading to a high thermal conductivity, and presents many defects causing low compressive strength and hardness. All the other foams present properties compliant to industrial standards, with a thermal conductivity λ of 24 mW m^{-1} K^{-1} or below, closed cells content above 95 %, cells diameters below 200 μm and compression strength above 300 kPa.

The polyol aromaticity does not positively influence the compressive strength, unlike expected for bulk polymers. Indeed, mechanical properties of the foams are not only influenced by the mechanical properties of the bulk polymer, but also by the foam density and pore distributions. Only the dimensional stability under wet conditions (70 °C, 90 %RH) seems to be correlated to the polyol aromaticity, as seen in Fig. 7. Since the polyol aromaticity and the density of ester bonds are inherently linked in the designed polyols, as seen from the FTIR analysis (Fig. 1c), it is more likely that increasing the density of ester linkages favors the water absorption under humid conditions, causing a higher deformation.

3.4. *Influence of polyester polyols type on the thermal stability and reaction to fire of PIR foams*

The thermal stability of the foams was first evaluated by TGA under inert atmosphere. Evolution of weight and derivative weight against temperature are provided in SI (Fig. S17). All the foams show a two-steps thermal degradation, with a main degradation around 300 °C and a second one around 600 °C. The residual mass at 700 °C increases with the polyol aromaticity (Fig. 8a), because of the ability of aromatic structures to form char. The $T_{95\%}$ is significantly lower in the presence of FR, because of the low degradation and volatilization temperature of TCPP (Fig. 8b) [40,41]. In the presence of FR, it increases with the polyol aromaticity before reaching a plateau, whereas in the absence of FR it

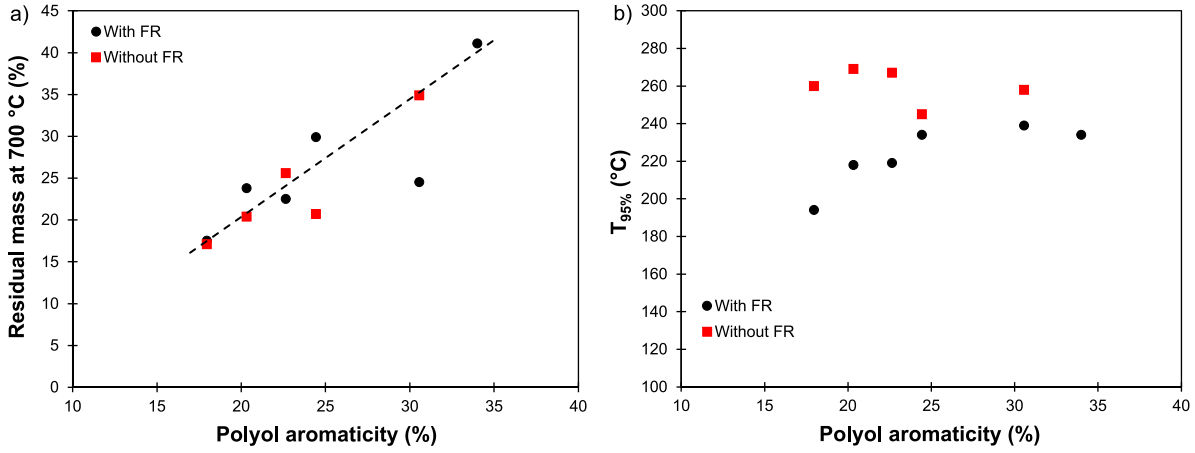

Fig. 8. (a) Residual mass at 700 °C and (b) $T_{95\%}$ measured by TGA (20 °C min^{-1} under helium), depending on the polyester polyol aromaticity.

Table 6
Flame height during flammability tests (EN 11925–2) of PIR foams prepared with the different polyester polyols.

Polyol	FR	Flame height (cm)
PA-MEG	yes	18
PA-DEG	yes	12
PA-TEG	yes	12
PA-PDO	yes	13
PA-DPDO	yes	13
PA-HDO	yes	13

appears independent on the polyol structure.

The reaction to fire of the PIR foams was then evaluated by two different tests. First, flammability was evaluated through single-flame source tests, according to EN ISO 11925–2 standard. In this test, a flame is directly applied to the sample, and the height of the resulting propagation is measured. The foam prepared with PA-MEG had a higher flame than the others, for which no significant difference could be noticed (Table 6). The higher value is probably caused by surface defects on the foam prepared with PA-MEG, as discussed above, rather than by differences related to the polyester polyol structure.

To gain deeper insights into the fire behavior of the foams, MLC tests were then performed. HRR curves are given in SI (Fig. S18), and the main results are gathered in Table 7. Two series of foams, prepared with or without FR, were tested. The influence of the FR appears clearly when comparing the results. For all the foams, it leads to an important decrease of pHRR and THR, as well as to an increase in the residual mass. However, it has no clear influence on the ignition time, flaming time and time to reach pHRR. The ignition times are short, between 3 and 7 s, and no significant differences between the different foams can thus be noticed. Short ignition times are characteristic of PUR and PIR foams, and are due to their low thermal inertia, which is a consequence of their low density and thermal conductivity [9]. Heat conduction into the foam being low, the surface of the material heats up quickly after exposure to the external heat flux, leading to a fast ignition.

To check whether the polyol aromaticity has an influence on the fire behavior, results of the MLC tests have been examined with respect to the polyol aromaticity. The corresponding plots, shown in the SI (Fig. S19), do not show any significant correlation between the fire behavior and the aromaticity.

As discussed in the introduction, the content in isocyanurate has already been recognized as the most important parameter affecting the fire behavior of PIR foams. Here, although the index was kept constant, differences in polyol reactivities have led to slight variations in the isocyanurate content, as revealed by FTIR analysis (Fig. 6c). The main results of the MLC tests have then been plotted against the intensity of the isocyanurate peak measured by FTIR, to check whether it can explain the behavior of the different foams. The results are shown in Fig. 9. In the absence of FR, both pHRR and THR tend to decrease when increasing the isocyanurate content. In the foams containing FR, there is only a slight decrease in pHRR and THR with the isocyanurate content. Surprisingly, the foam prepared with the polyol PA-HDO appears far from the trend observed for the other foams, with significantly higher values of both pHRR and THR. It also shows a much lower residual mass, only 16.7 % against 43–47 % for the other foams.

Some authors have mentioned the elemental composition of the polyols as an impactful parameter to understand the reaction to fire, a higher content in hydrogen being associated to a higher flammability [10]. Elemental analysis was thus performed to determine the content in

Table 8
Elemental analysis of the polyester polyols.

Polyol	C (%)	H (%)	O (%)
PA-MEG	58.90	5.01	36.10
PA-DEG	57.14	6.21	36.66
PA-TEG	55.33	6.94	37.74
PA-PDO	61.28	5.84	32.88
PA-DPDO	60.21	7.35	32.45
PA-HDO	65.74	8.03	26.24

Table 7
Results of MLC tests carried out at 35 kW m^{-2} external heat flux.

Foam series	Polyol	$t_{ignition}$ (s)	$t_{flaming}$ (g)	pHRR (kW/m^{-2})	t_{pHRR} (s)	THR (MJ/m^{-2})	$m_{residual}$ (%)
with FR	PA-MEG	7	82	56.1	35	2.61	47.2
	PA-DEG	6	107	47.2	24	2.14	43.0
	PA-TEG	5	80	51.0	20	1.96	43.4
	PA-PDO	7	66	51.4	26	2.45	45.7
	PA-DPDO	5	101	54.2	23	2.44	46.3
	PA-HDO	5	94	78.5	36	5.72	16.7
without FR	PA-DEG	4	114	104.8	30	6.99	15.1
	PA-TEG	5	106	100.1	46	6.72	26.7
	PA-PDO	4	68	161.3	35	8.11	27.5
	PA-DPDO	4	92	112.5	28	7.37	18.4
	PA-HDO	6	91	133.6	33	9.60	23.2

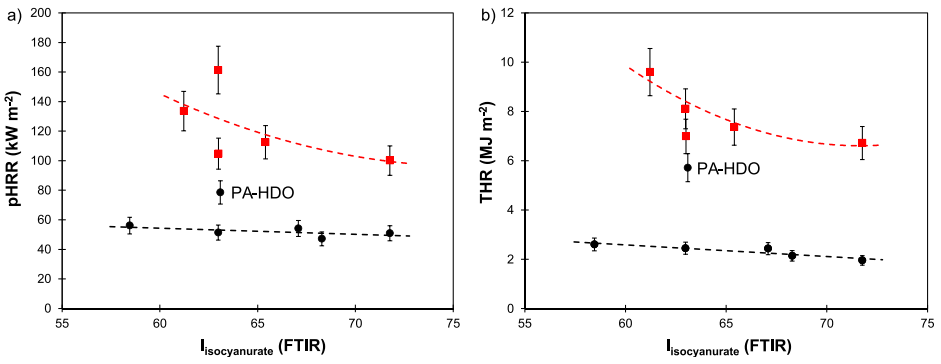

Fig. 9. Evolution of (a) pHRR and (b) THR of the different foams, depending on the intensity of the isocyanurate peak measured by FTIR.

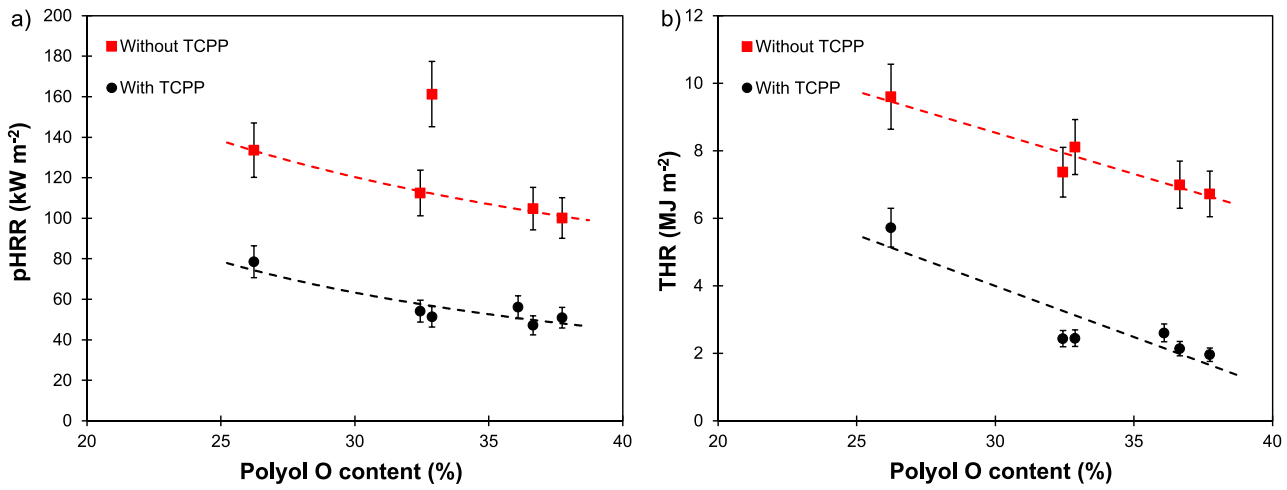

Fig. 10. Evolution of (a) pHRR and (b) THR of the different foams, depending on the O content of the polyester polyols.

C, O and H of the polyols (Table 8). PA-HDO has indeed the highest H content of the polyols, which could explain the higher flammability of the resulting foam. However, pHRR and THR don't increase with the H content, but U-shaped curves are rather observed (Fig. S20). The content in O of the polyols seems to be a better indicator of the foams fire behavior. Both pHRR and THR decrease when the O content of the polyols increases, with or without FR (Fig. 10). It thus seems to be a key parameter influencing the flammability. This is probably related to a better char-forming ability, which leads to the formation of a dense protective layer that prevents exposition of the polymer to the flame. Less efficient char formation for the foam prepared with polyol PA-HDO could also explain the low residual mass. The polyol atomic composition thus seems more important than its aromaticity when it comes to explaining the fire resistance of PIR foams.

4. Conclusions

A series of 6 polyester polyols was synthesized by reaction between PA and various short diols, while maintaining a constant I_{OH} of the final polyester polyols. Increasing the molar mass of the diols leads to a decrease in the polyester polyols aromaticity and density of ester bonds. The macromolecular architecture has strong consequences on T_g and viscosity, which both significantly increase with the aromaticity.

The polyols were used to synthesize PIR foams with a constant index of 320. Increasing polyester polyol aromaticity reduces the molecular mobility, which causes slower foaming kinetics. Besides, slight variations in isocyanurate content were observed depending on the temperature reached during foaming. The aromaticity does not significantly impact the foams' structure and properties, and unlike often mentioned was not found to positively influence the reaction to fire of the PIR foams. However, two parameters were found to be impactful. Firstly, an increase in the isocyanurate content reduces pHRR and THR, especially in the absence of FR. Secondly, pHRR and THR were shown to decrease with increasing oxygen content in the polyols. It means that in combination with the presence of isocyanurate linkages and aromatic structures, a higher oxygen content leads to improved reaction to fire. It is assigned to a better charring ability, which leads to the formation of a dense layer that protects the polymer from degradation.

This systematic study thus clearly shows that to improve the reaction to fire of PIR foams, the polyol aromaticity should not be considered as only key factor. It seems more important to focus on formulations allowing to maximize the formation of isocyanurate at a given index, and to select polyols with a high content in oxygen. Further works on polyester polyols with different chemical structures, including fully aliphatic ones, should now be conducted to complement this study.

CRediT authorship contribution statement

Antoine Duval: Writing – review & editing, Writing – original draft, Supervision, Methodology, Investigation, Formal analysis, Conceptualization. **Johan Sarazin:** Writing – review & editing, Investigation, Formal analysis. **Cecile de Haas:** Investigation, Formal analysis. **Alexandru Sarbu:** Writing – review & editing, Methodology, Funding acquisition, Conceptualization. **Serge Bourbigot:** Writing – review & editing, Supervision, Resources, Formal analysis. **Luc Avérous:** Writing – review & editing, Supervision, Resources, Funding acquisition.

Declaration of competing interest

The authors declare that they have no known competing financial interests or personal relationships that could have appeared to influence the work reported in this paper.

Data availability

Data will be made available on request.

Acknowledgments

We acknowledge the Cronenbourg NMR Core Facility (CNRS/Université de Strasbourg, UMR 7042 LIMA, Strasbourg, France) for the ^{1}H and ^{31}P NMR spectra acquisition. Isabelle Dhenin and William René (Soprema) are thanked for their help with the foam preparation and characterization. AD, AS and LA acknowledge funding from Agence Nationale de la Recherche (ANR) for the project MIPLACE within the framework of the ERA-CoBioTech program of the EU.

References

[1] International Energy Agency, World Energy Balances – Analysis. https://www.iea.org/reports/world-energy-balances-overview, 2021 (accessed 28 July 2021).
[2] S. Schiavoni, F. D'Alessandro, F. Bianchi, F. Asdrubali, Insulation materials for the building sector: a review and comparative analysis, Renew. Sustain. Energy Rev. 62 (2016) 988–1011, https://doi.org/10.1016/j.rser.2016.05.045.
[3] W. Villasmil, L.J. Fischer, J. Worlitschek, A review and evaluation of thermal insulation materials and methods for thermal energy storage systems, Renew. Sustain. Energy Rev. 103 (2019) 71–84, https://doi.org/10.1016/j.rser.2018.12.040.
[4] E. Delebecq, J.-P. Pascault, B. Boutevin, F. Ganachaud, On the versatility of urethane/urea bonds: reversibility, blocked isocyanate, and non-isocyanate polyurethane, Chem. Rev. 113 (2013) 80–118, https://doi.org/10.1021/cr300195n.
[5] S.T. McKenna, N. Jones, G. Peck, K. Dickens, W. Pawelec, S. Oradei, S. Harris, A. A. Stec, T.R. Hull, Fire behaviour of modern façade materials – understanding the

grenfell tower fire, J. Hazard. Mater. 368 (2019) 115–123, https://doi.org/10.1016/j.jhazmat.2018.12.077.
[6] G. Mitchener, Impact of Grenfell Tower fire disaster on polyisocyanurate industry, Polimery 63 (2018) 716–722. 10.14314/polimery.2018.10.8.
[7] P.I. Kordomenos, J.E. Kresta, Thermal stability of isocyanate-based polymers. 1. kinetics of the thermal dissociation of urethane, oxazolidone, and isocyanurate groups, Macromolecules 14 (1981) 1434–1437, https://doi.org/10.1021/ma50006a056.
[8] C. Dick, E. Dominguez-Rosado, B. Eling, J.J. Liggat, C.I. Lindsay, S.C. Martin, M. H. Mohammed, G. Seeley, C.E. Snape, The flammability of urethane-modified polyisocyanurates and its relationship to thermal degradation chemistry, Polymer 42 (2001) 913–923, https://doi.org/10.1016/S0032-3861(00)00470-5.
[9] M. Günther, A. Lorenzetti, B. Schartel, Fire phenomena of rigid polyurethane foams, Polymers 10 (2018) 1166, https://doi.org/10.3390/polym10101166.
[10] M.J. Skowronski, A. DeLeon, Isocyanurate foam the role of the polyol, J. Cell. Plast. 15 (1979) 152–157, https://doi.org/10.1177/0021955X7901500304.
[11] M.K. Laughner, J.M. Gross, D.W. Baugh, New polyol development in rigid hybrid polyurethane/polylsocyanurate foam systems, J. Cell. Plast. 19 (1983) 182–188, https://doi.org/10.1177/0021955X8301900309.
[12] S.B. Burns, E.L. Schmidt, The PIR/PUR ratio: a novel Timer conversion test with high Correlation to the factory mutual calorimeter for HCFC-141b blown Polyisocyanurate foams, J. Cell. Plast. 31 (1995) 137–153, https://doi.org/10.1177/0021955X9503100204.
[13] S.V. Levchik, E.D. Weil, Recent Progress in flame Retardancy of polyurethane and Polyisocyanurate foams, in: C.A. Wilkie, G.L. Nelson (Eds.), Fire and Polymers IV, American Chemical Society, Washington, 2005, pp. 280–290, https://doi.org/10.1021/bk-2006-0922.ch022.
[14] B. Czupruński, J. Paciorek-Sadowska, J. Liszkowska, The effect of tri(1-chloro-3-etoxy-propane-2-ol) borate on the properties of rigid polyurethane-polyisocyanurate foams, Polimery 47 (2002) 727–729.
[15] M. Borowicz, J. Paciorek-Sadowska, J. Lubczak, B. Czupryński, Biodegradable, flame-Retardant, and bio-based rigid Polyurethane/Polyisocyanurate foams for thermal insulation application, Polymers 11 (2019) 1816, https://doi.org/10.3390/polym11111816.
[16] M. Modesti, A. Lorenzetti, F. Simioni, M. Checchin, Influence of different flame retardants on fire behaviour of modified PIR/PUR polymers, Polym. Degrad. Stab. 74 (2001) 475–479, https://doi.org/10.1016/S0141-3910(01)00171-9.
[17] W. Zatorski, Z.K. Brzozowski, K. Łebek, Production of PUR and PUR-PIR foams with red phosphorus as a flame retardant, Polimery 50 (2005) 686–689.
[18] Y. Liu, J. He, R. Yang, The preparation and properties of flame-retardant polyisocyanurate–polyurethane foams based on two DOPO derivatives, J. Fire Sci. 34 (2016) 431–444, https://doi.org/10.1177/0734904116662667.
[19] X. Qian, Q. Liu, L. Zhang, H. Li, J. Liu, S. Yan, Synthesis of reactive DOPO-based flame retardant and its application in rigid polyisocyanurate-polyurethane foam, Polym. Degrad. Stab. 197 (2022) 109852, https://doi.org/10.1016/j.polymdegradstab.2022.109852.
[20] M. Modesti, A. Lorenzetti, Flame retardancy of polyisocyanurate–polyurethane foams: use of different charring agents, Polym. Degrad. Stab. 78 (2002) 341–347, https://doi.org/10.1016/S0141-3910(02)00184-2.
[21] M. Modesti, A. Lorenzetti, F. Simioni, G. Camino, Expandable graphite as an intumescent flame retardant in polyisocyanurate–polyurethane foams, Polym. Degrad. Stab. 77 (2002) 195–202, https://doi.org/10.1016/S0141-3910(02)00034-4.
[22] M. Modesti, A. Lorenzetti, Improvement on fire behaviour of water blown PIR–PUR foams: use of an halogen-free flame retardant, Eur. Polym. J. 39 (2003) 263–268, https://doi.org/10.1016/S0014-3057(02)00198-2.
[23] M. Kurańska, U. Cabulis, M. Auguścik, A. Prociak, J. Ryszkowska, M. Kirpluks, Bio-based polyurethane-polyisocyanurate composites with an intumescent flame retardant, Polym. Degrad. Stab. 127 (2016) 11–19, https://doi.org/10.1016/j.polymdegradstab.2016.02.005.
[24] Y. Liu, J. He, R. Yang, The effects of aluminum hydroxide and ammonium polyphosphate on the flame retardancy and mechanical property of polyisocyanurate–polyurethane foams, J. Fire Sci. 33 (2015) 459–472, https://doi.org/10.1177/0734904115609362.
[25] Y. Liu, J. He, R. Yang, Effects of dimethyl methylphosphonate, aluminum hydroxide, ammonium polyphosphate, and expandable graphite on the flame Retardancy and thermal properties of Polyisocyanurate-polyurethane foams, Ind. Eng. Chem. Res. 54 (2015) 5876–5884, https://doi.org/10.1021/acs.iecr.5b01019.
[26] E. Asimakopoulou, J. Zhang, M. Mckee, K. Wieczorek, A. Krawczyk, M. Andolfo, T. Kozlecki, M. Scatto, M. Sisani, M. Bastianini, A. Karakassides, P. Papakonstantinou, Effect of layered double hydroxide, expanded graphite and ammonium polyphosphate additives on thermal stability and fire performance of polyisocyanurate insulation foam, Thermochim Acta 693 (2020) 178724, https://doi.org/10.1016/j.tca.2020.178724.
[27] L. Gao, G. Zheng, Y. Zhou, L. Hu, G. Feng, M. Zhang, Synergistic effect of expandable graphite, diethyl ethylphosphonate and organically-modified layered double hydroxide on flame retardancy and fire behavior of polyisocyanurate-polyurethane foam nanocomposite, Polym. Degrad. Stab. 101 (2014) 92–101, https://doi.org/10.1016/j.polymdegradstab.2013.12.025.
[28] W. Zatorski, Z.K. Brzozowski, A. Kolbrecki, New developments in chemical modification of fire-safe rigid polyurethane foams, Polym. Degrad. Stab. 93 (2008) 2071–2076, https://doi.org/10.1016/j.polymdegradstab.2008.05.032.
[29] M. Modesti, A. Lorenzetti, Halogen-free flame retardants for polymeric foams, Polym. Degrad. Stab. 78 (2002) 167–173, https://doi.org/10.1016/S0141-3910(02)00130-1.
[30] Q. Xu, T. Hong, Z. Zhou, J. Gao, L. Xue, The effect of the trimerization catalyst on the thermal stability and the fire performance of the polyisocyanurate-polyurethane foam, Fire Mater. 42 (2018) 119–127, https://doi.org/10.1002/fam.2463.
[31] J. Lenz, D. Pospiech, M. Paven, R.W. Albach, B. Voit, Influence of the catalyst concentration on the chemical structure, the physical properties and the fire behavior of rigid polyisocyanurate foams, Polym. Degrad. Stab. 177 (2020) 109168, https://doi.org/10.1016/j.polymdegradstab.2020.109168.
[32] J. Reignier, F. Méchin, A. Sarbu, Chemical gradients in PIR foams as probed by ATR-FTIR analysis and consequences on fire resistance, Polym. Test. 93 (2021) 106972, https://doi.org/10.1016/j.polymertesting.2020.106972.
[33] J.S. Canaday, M.J. Skowronski, A Comparison of aromatic polyester polyols for rigid urethane and isocyanurate foam, J. Cell. Plast. 21 (1985) 338–344, https://doi.org/10.1177/0021955X8502100507.
[34] E. Dominguez-Rosado, J.J. Liggat, C.E. Snape, B. Eling, J. Pichtel, Thermal degradation of urethane modified polyisocyanurate foams based on aliphatic and aromatic polyester polyol, Polym. Degrad. Stab. 78 (2002) 1–5, https://doi.org/10.1016/S0141-3910(02)00086-1.
[35] A. Granata, D.S. Argyropoulos, 2-Chloro-4,4,5,5-tetramethyl-1,3,2-dioxaphospholane, a reagent for the accurate determination of the uncondensed and condensed phenolic moieties in lignins, J. Agric. Food Chem. 43 (1995) 1538–1544, https://doi.org/10.1021/jf00054a023.
[36] X. Meng, C. Crestini, H. Ben, N. Hao, Y. Pu, A.J. Ragauskas, D.S. Argyropoulos, Determination of hydroxyl groups in biorefinery resources via quantitative 31 P NMR spectroscopy, Nat. Protoc. 14 (2019) 2627–2647, https://doi.org/10.1038/s41596-019-0191-1.
[37] V. Babrauskas, Characteristics of external ignition source, in: V. Babrauskas (Ed.), Ignition Handbook, Fire Science Publishers, Issaquah (WA), 2003, pp. 497–590.
[38] B. Schartel, T.R. Hull, Development of fire-retarded materials—Interpretation of cone calorimeter data, Fire Mater. 31 (2007) 327–354, https://doi.org/10.1002/fam.949.
[39] P. Furtwengler, R. Matadi Boumbimba, A. Sarbu, L. Avérous, Novel rigid Polyisocyanurate foams from synthesized biobased polyester polyol with enhanced properties, ACS sustainable Chem. Eng. 6 (2018) 6577–6589, https://doi.org/10.1021/acssuschemeng.8b00380.
[40] I. van der Veen, J. de Boer, Phosphorus flame retardants: properties, production, environmental occurrence, toxicity and analysis, Chemosphere 88 (2012) 1119–1153, https://doi.org/10.1016/j.chemosphere.2012.03.067.
[41] D. Xu, K. Yu, K. Qian, Effect of tris(1-chloro-2-propyl)phosphate and modified aramid fiber on cellular structure, thermal stability and flammability of rigid polyurethane foams, Polym. Degrad. Stab. 144 (2017) 207–220, https://doi.org/10.1016/j.polymdegradstab.2017.08.019.